Journal of Visualization, Vol. 7, No. 1 (2004) 9-16

Quantitative Visualization of Micro-Tube Flow Using Micro-PIV

Sugii, Y. *[1] and Okamoto, K. *[2]

*1 Nuclear Engineering Research Laboratory, University of Tokyo,Tokai-mura, Ibaraki, 319-1188, Japan. E-mail: sugii@utnl.jp
*2 Nuclear Engineering Research Laboratory, University of Tokyo,Tokai-mura, Ibaraki, 319-1188, Japan.

Received 28 February 2003
Revised 29 July 2003

Abstract : This paper describes PIV measurements of the flow field in a micro round tube with an internal diameter of 100 μm in order to examine micro-scale effects. Since the refractive index of the micro tube almost corresponds to that of water, the inner flow in the tube can be observed clearly. The micro PIV system has been developed using a microscope, a high sensitive CCD camera, a double pulsed Nd:YAG laser and optics. Applying the micro PIV technique to the flow, the velocity distributions with spatial resolution of 1.8 × 1.8 μm were measured even near the wall in the center plane of the round tube. It was found that the velocities near the tube wall were smaller than the theoretical values calculated by using Poiseuille's law. It is believed that this disparity is due to micro-scale effects such as interference between particles and the wall, friction at the wall, surface tension and so on.

Keywords : Micro PIV, Fluorescent particle, Round tube

1. Introduction

Microcirculation, which occurs in arterioles, capillaries and venules with diameters from 5 to 50 μm, is essential in the process of maintaining healthy tissues and organs. Particularly to measure the velocity with high spatial resolution and highly measurement accuracy is crucial for the scientific and clinical study in evaluating deliberation to the tissues and organs of the body and shear stress of blood cells and endothelial cells. A number of investigations of the velocity field, using the ultrasonic Doppler flowmeter, laser Doppler velocimetry, the dual slit method and so on, have been reported (Wayland et al 1967, Intaglietta et al 1975, Cochrane et al 1981, Seki 1996, Tangelder et al 1986, Yamaguchi et al 1992, Bishop et al 2001). The flow features for non-Newtonian fluid were observed. The authors have also developed the highly accurate PIV technique (Sugii et. al., 2000), which can improve measurement accuracy and spatial resolution, and applied it to the blood flow images with a diameter of 30 μm arteriole using an intravital-microscope and the high-speed digital video system (Nakano et al., 2001, Sugii et. al., 2001). The result showed that the dynamics was complex because of micro scale effect, multi-phase flow, non-Newtonian fluid, the cardiac cycle and non-uniform geometry.

Conversely, significant attention has been given to micro flow due to the development in micro fluidic devises. It was reported that the flows in micro scale was different from the flows in macro scale because some factors were normally neglected in conventional macro flow (Ho and Tai 1998). In micro flow, surface forces dominate the flow because of larger surface area-to-volume ratio. Meta and Li (1999) have proposed that surface roughness increases the momentum transfer in boundary layer near the wall. Several researchers have suggested the possibility of slip at the wall for a liquid fluid on a surface (Watanabe at al 1998, Barrat et al 1999, Pit et al 2000). Recently so-called micro PIV techniques, using a microscope and a CCD camera, have been developed to investigate the flow behaviors in a micro fluidic device. Santiago et al. (1998) used the conventional PIV technique with an epi-fluorescent microscope with a continuous lamp and an intensified CCD camera (Princeton instrument) to record the flow around a diacylinder of 30 μm diameter seeded with 300 nm diameter particles. Meinhart et al. (1999) used a pulsed Nd:YAG laser and a cooled interline transfer CCD camera to measure the flow field in a 30 μm × 300 μm × 25 mm rectangular microchannel seeded with 200 nm diameter particles. Koutsiaris et al. (1999) measured the flow field inside glass capillaries with internal diameters of approximately 200 μm seeded with 10 μm diameter particle. However, these measurement results have corresponded with Poiseuille's velocity profile, which is a theoretical solution of a Laminar flow with no-slip boundary condition.

In this paper, in order to clarify the dynamics of microcirculatory blood flow, the micro-PIV technique is applied to the pressure-driven flow in a micro round tube. Micro-scale effects were investigated in a micro round tube of internal diameter 100 μm with a refractive index corresponding to that of water, using a microscope with a water-immersion objective lens.

2. Experimental Setup and Method

2.1 Experimental Setup

An inner flow of the micro round tube taken instead of a rectangular micro channel was used to investigate the micro-scale effects of microcirculation. Usually in the case of a round tube, since light was refracted by the curvature due to difference of refractive index between the tube material made of glass plastic, and fluid, it was difficult to observe an inner flow and especially near the wall. In this experiment, the tube was made of FEP (Fluorinated Ethylene Polymer), with inner and outer diameters of 100 μm and 300 μm, respectively. Figure 1 shows a schematic view of experimental set up. The refractive index of the tube is 1.338, almost equal to that of water 1.33. Ion-exchange water was used as working fluid and the tube was dipped in water. By the observation under a con-focal microscope filling up with fluorescence particles in the tube, it was confirmed that the refraction at the tube wall was negligibly small and the flow inside the tube, significantly very close to wall, could be observed clearly. A water-immersion objective lens with long working distance W.D. = 3.3 mm, a magnification M = 40 and a numerical aperture N.A. = 0.8 was used. The backlight illumination instead of epi-illumination was taken in order to improve the image quality by reducing spatial unevenness of illumination. Since in the case of epi-illumination, a filter cube composed of a dichroic mirror, a high-pass filter and low-pass filter were needed, fluorescent light was reduced. Conversely, since only one filter was used in the backlight illumination, the image quality was also improved. The micro tube was mounted in a horizontal position in a laboratory dish filled with water. The laser beam was illuminated from downside of the microscopic stage. The illuminating beam was produced by a continuous Nd:YAG laser, wavelength λ = 532 nm. A fluorescent particle with diameters of 1 μm absorbs green light (peak wavelength 542 nm) and emits red light (peak wavelength 612 nm). The light emitted by the fluorescent particles was captured through a water-immersion objective lens. The particle image was recorded using a cooled CCD camera equipped optical filter λ = 550 nm. The images consisted of 1280 × 1024 pixels with 12 bit gray levels at a rate of 8 frames/sec and 64 pair images can be stored. A syringe pump with 100 μL capacity was used to force the liquid through micro tube at constant flow rate, 200, 100, 50 and 25 μL/h. The maximum velocities at the center of the tube corresponded with about 18, 9, 4.5 and 2.25 mm/sec, respectively. By controlling time interval between double pulse laser illuminations from 100 to 800 μsec, image displacement was adjusted to about 10 pixel/frame at every flow rate. The experimental and optical conditions of the micro PIV system were shown in Table 1 and Table 2. The depth of focus δz of a microscope objective lens has been proposed (Meinhart et al., 2000a). The depth of focus δz is about 6 % of the tube diameter.

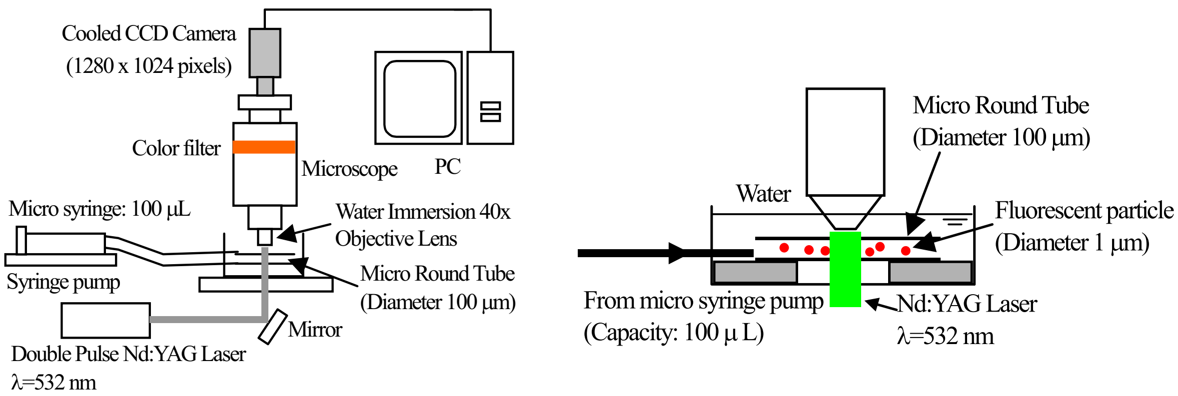

(a) Side view showing the optical system (b) Geometry of the objective lens and test section

Fig. 1. Schematic view of the micro PIV system.

Table. 1. Experimental Condition

Inner diameter of microtube	100 μm
Refractive index of microtube	1.338
Flow rate	25 - 200 μL/h
Maximum velocity	2.25 - 18.0 mm/sec
Reynolds number	0.113 - 0.9
Particle concentration	0.4 % solids
Particle density	1.05 g/cm^3

Table. 2. Optical Condition

N.A.	0.8
Resolution	0.18 μm/pixel
Particle diameter d_p	1.0 μm
Particle diameter d_e on CCD plane	43.0 μm
Particle diameter d_e/size of CCD cell	5.8 pixel
Depth of focus δz	6.2 μm

2.2 Analysis Method

Figure 2 shows a captured fluorescent particle image in a micro tube illuminated by Nd:YAG laser and halogen light with the focal plane set to be at the center of the micro round tube. The observed region was 231 × 184 μm in size, with each pixel representing a 0.18 × 0.18 μm area. Particles appear in Fig. 2 (a) as bright point sources of light were randomly distributed through the tube. Background noise was due to out-of-focus particles and the light scattering caused by tube wall. The wall in the center plane of the tube can be recognized in the upper and lower part of the image. Since the refraction index of the tube in this study corresponds to that of water, particles near the wall can be observed clearly. A particle diameter in image was observed as 7 or 8 pixels with low particle density. In Fig.2 (b), the flow is visualized using back light illumination by a halogen light from the bottom. The wall in the center plane of the tube can be recognized in the upper and lower part of the image.

Under a microscopic observation, particle diameter in image becomes larger and particle

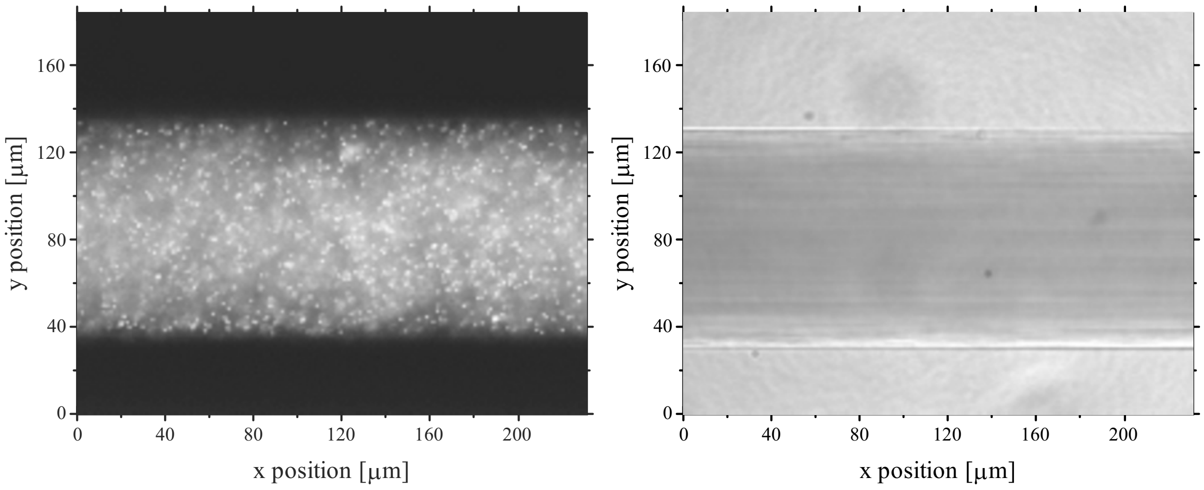

(a) Illuminated by Nd:YAG laser (b) Illuminated by halogen light

Fig. 2. Visualized images in the center plane of the micro round tube.

density becomes very smaller. Therefore, the measurement accuracy was reduced using a conventional PIV technique, which consists of the combination of cross-correlation method and Gaussian peak fit for sub-pixel analysis. Recently to improve the measurement accuracy for time-averaging velocity distribution, averaging instantaneous correlation functions technique was proposed (Meinhart et al., 2000b). However, it is difficult to obtain time-series velocity and temporal variance due to Brownian motion, interaction between particle and wall and so on. The authors have also developed the highly accurate PIV technique (Sugii et. al., 2000), which can improve measurement accuracy and spatial resolution. It was reported that the errors of the method were smaller with larger particle diameters even in very low particle density than those of the Gaussian fit. The measurement precision and reliability are usually evaluated by comparing the results with the given displacements to analyze the synthetic images, such as PIV standard images (Okamoto et al., 2000). In order to access effect of fluorescent particle image in micro PIV, the method was applied to the synthetic image with almost the same condition as the experiment. Particle image was generated with Poiseuille's velocity profile for the round tube; a maximum displacement in x direction set to be 10 pixel /frame at the center of the tube, and the velocities at the wall with the tube diameter of 550 pixels become zero, and all of the velocities in y direction and z direction set to be zero. Particle diameter and density set to be 7 pixels and 5 particles per 33 × 33 pixel window, respectively. The individual particle was described with the Gaussian intensity profile at a randomly distributed location in space. The image size was 1280 × 1024 pixels with maximum intensity 200 gray levels. Figure 3 shows averaged displacement profile and RMS error of 100 velocities obtained by the present method and Gaussian peak fit, in which correlation coefficients were obtained using direct cross-correlation method. The interrogation windows of the present method and Gaussian peak fit were taken as 21 × 21 and 33 × 33 pixels with 50% overlap, respectively. The averaged profiles of both methods agreed with Poiseuille's profile. However, the RMS errors of the present method even with smaller interrogation window were smaller than that of Gaussian fit. RMS errors of the present method were almost constant and smaller than 0.5 pixels, especially that at the maximum displacement was zero. RMS errors of the Gaussian fit were shown larger around y = 100, 500 due to low particle density and displacement gradient. In contrast, in the present method, they disappeared. The results show usefulness of the present method for fluorescent particle image in micro scale.

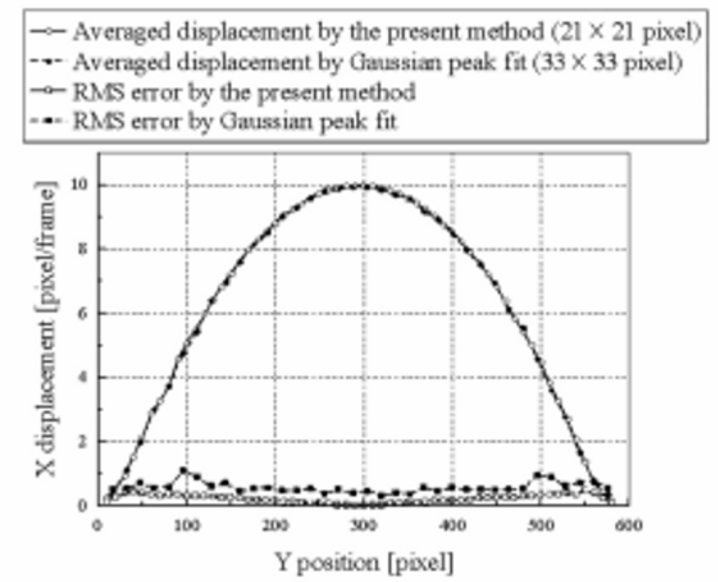

Fig. 3. Axial displacement profiles and RMS error for synthetic image.

3. Results and Discussion

Figure 4 shows the time-averaged velocity distributions of 64 maps for 16 sec in the microtube at 200 μl/h flow rate, calculated using the PIV technique described in the previous section. An interrogation window of 21 × 21 pixels was taken with 50% overlap, corresponding to a spatial resolution of 1.8 × 1.8 μm. The velocities in the horizontal direction were thinned out for clarity. The maximum velocity was about 10.0 pixels/frame or 18.0 mm/sec at the center of the tube. Spurious vectors were not observed in the velocity distribution—it looks like a typical laminar flow. Velocity vectors out of flow region were zero because of eliminating background noise. The velocity vectors very close to the wall were measured and it was found that the wall-normal component of the velocity vectors is close to zero, because the micro round tube flow is fully developed. Pulsation of flow due to syringe pump was small enough.

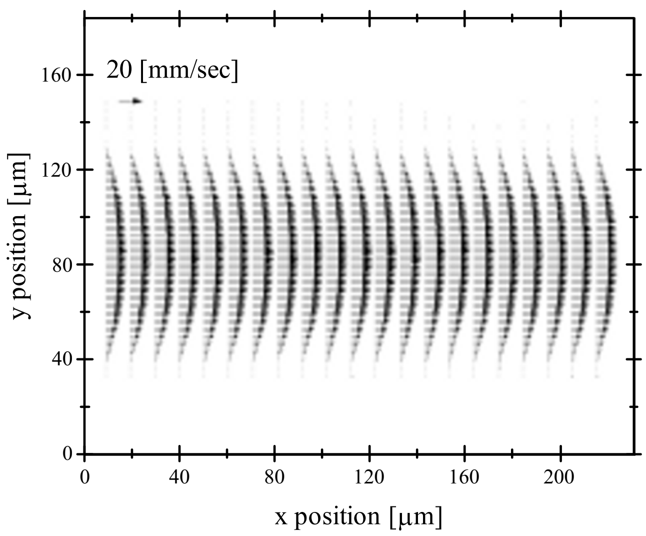

Fig. 4. Time-averaged velocity distribution in microtube.

Figure 5 shows the axial velocity profiles and temporal variance of the vertical section in Fig.4. The results obtained by the Gaussin peak fit with an interrogation window of 33 × 33 pixels with 50% overlap, were represented as a dotted line. Fifty-five velocity values in results of the present method were obtained along the capillary diameter at spacing of 1.8 μm. As noted above it was found that the velocity vectors near the wall could be measured. The averaged profiles of both methods were similar. However, the variance of the present method even with a smaller interrogation window was quite smaller than that of the Gaussian fit. These variances of the present method were larger than the results of the synthetic image in Fig.3. It was considered that the image was spoiled by noise due to out-of-focus particles. In principle, a Newtonian fluid of laminar flow in a round tube has a velocity distribution conforming to Poiseuille's law. The theoretical velocity distribution was shown in Fig.5 as a red line. Both of the profiles around the center corresponded closely to the theoretical profile. However, the velocities near the wall obtained by both methods were slightly smaller than the theoretical values. These variances of both methods were significantly larger near the wall region compared with these values around the center.

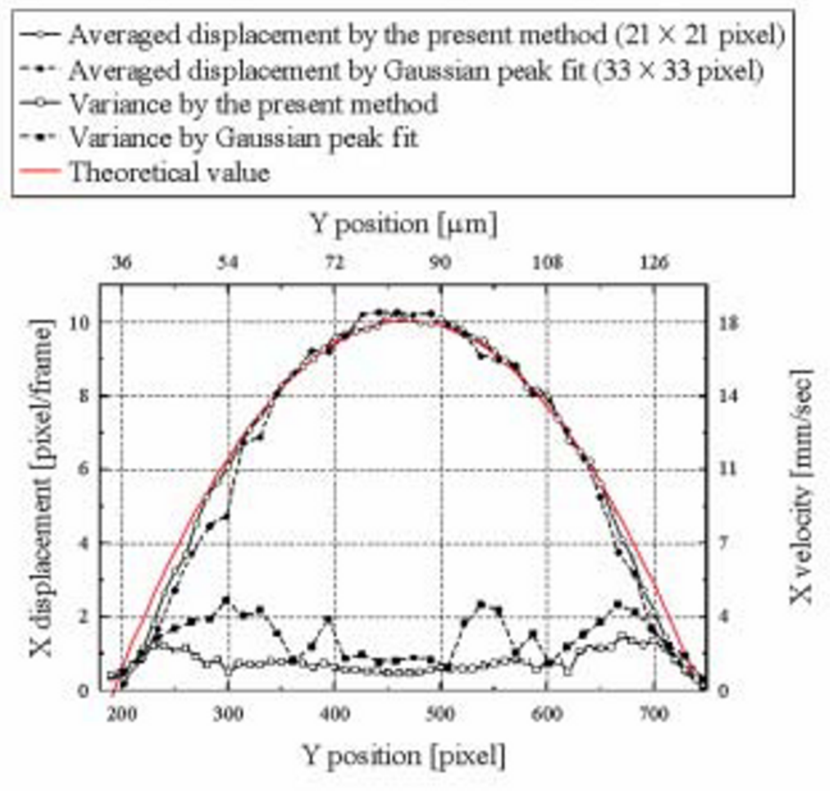

Fig. 5. Axial velocity displacement and variance profiles.

Figure 6 shows the axial velocity profiles and temporal variance obtained by the PIV method varying maximum velocity from 18.0 to 2.25 mm/sec. The position, velocity and variance were normalized using the radius of the tube and each maximum velocity, respectively. Theoretical profile was also shown in the figure. These profiles around the center corresponded closely to the theoretical profile. These velocities near the wall were slightly smaller than the theoretical value even with different Reynolds numbers. Although all of the differences between the experimental results and theoretical results are within 10 % around the center, the experimental results show about 60% of theoretical values around r = ± 0.9. Temporal variances were very similar in all cases. These variances near the wall, around r = ± 0.8, increased. These variances near the wall in all cases similarly doubled around the center. The experimental results of two sets for each case show same results, resulting in confirmation of reproducibility.

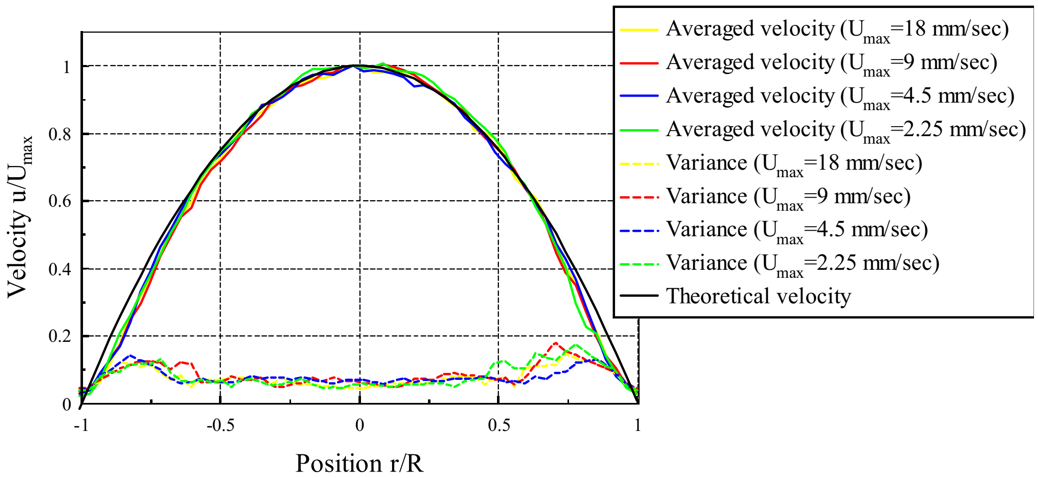

Fig. 6. Axial velocity displacement and variance profiles varying maximum velocity normalized using the radius of the tube and the each maximum velocity.

Since the refractive indices of water and tube were 1.33 and 1.338, respectively, the effect of refraction due to the roundness of the tube was small enough to be rejected as a source of this deviation. Although the measured velocity was a weighted average over the depth of the fluid (Olsen et. al., 2000), the depth of field 6.2 μm shown in Table 2 was small compared with the velocity gradient in the depth direction. A mean square distance of diffusion cased by Brownian motion is given by,

$$\left\langle s^2 \right\rangle = \frac{2\kappa T}{3\pi\mu d_p}\Delta t \tag{1}$$

Here, d_p is the particle diameter, κ is Boltzman's constant, T is the absolute temperature of the fluid, μ is the dynamic viscosity of the fluid and Δt is time interval between double pulse lasers.

The mean square distance of diffusion was estimated as 0.0046 to 0.013 μm. Since these values were smaller than 0.1 pixel, the influence of it can be ignored. Since heating caused by laser illumination was also small enough, the tube was dipped in a mount of water. Therefore, it is believed that the deviation of the velocities from the theoretical value near the wall is not based on error in measuring the velocity gradient, depth of field. Possible causes are interference between particles and the wall, friction at the wall, surface tension and so on. The water contact angle, adhesion force and coefficient of dynamic friction of FEP, the tube material, are 115 degree, 42 dyne/cm and 0.3, respectively. Therefore, the tube surface is very slippery compared with glass or acrylic resin. It is considered that the particle collides with the inner wall of tube or is affected by electrostatic force caused by the charged surface.

4. Conclusion

Micro-scale effects of a flow in a microtube varying Reynolds number were examined using the micro PIV technique. Applying the PIV technique to the flow field in a micro round tube with internal diameter of 100 μm, the velocity distributions with a spatial resolution of 1.8 × 1.8 μm were measured even near the wall in the center plane of the round tube. Since the refractive index of the micro tube almost corresponds to that of water, the inner flow in the tube can be observed clearly and velocity very close to the wall can be measured. The results showed that the deviation of the obtained velocities from the theoretical value calculated using Poiseuille's law and larger variance near the wall. This effect is believed to be due to micro-scale effects such as interference between particles and the wall, friction at the wall, surface tension.

References

Barrat, J. L. and Bocquet, L., Large Slip Effect at a Nonwetting Fluid-Solid Interface, Physical Review Letters, 82-23 (1999), 4671-4674.

Bishop, J. J., Nance, P. R., Popel, A. S., Intaglietta, M. and Johnson, P. C., Effect of Erythrocyte Aggregation on Velocity Profiles in Venules, Am. J. Physiol. Heart Circ. Physiol., 280 (2001), H222-H236.

Cochrane, T., Earnshaw, J. C. and Love, A. H. G., Laser Doppler Measurement of Blood Velocity in Microvessels, Med. & Biod. Eng. & Comput., 19-15 (1981), 589-596.

Keane, R. D. and Adrian, R. J., Theory of Cross-Correlation Analysis of PIV, Applied Scientific Research, 49-3 (1992), 191-215.

Koutsiaris, A. K., Mathioulakis, D. S. and Tsangaris, S., Microscope PIV for Velocity-field Measurement of Particle Suspensions Flowing Inside Glass Capillaries, Meas. Sci. Technol., 10 (1999), 1037-1046.

Ho, C. M. and Tai, Y. C., Micro-Electro-Mechanical Systems (MEMS) and Fluid Flows, Annual Review of Fluid Mechanics, 30 (1998), 579-612.

Intaglietta, M., Silverman, N. R. and Tompkins, W. R., Capillary Flow Velocity Measurements in Vivo And in Situ by Television Methods, Microvasc. Res., 10 (1975), 165-179.

Mala, G. M. and Li, D., Flow Characteristics of Water in Microtubes, International Journal of Heart and Fluid Flow, 20 (1999), 142-148.

Meinhart, C. D., Wereley, S. T. and Santiago, J. G., PIV Measurement of a Microchannel Flow, Exp. Fluids, 27 (1999), 414-419.

Meinhart, C. D., Wereley, S. T. and Gray, M. H. B., Volume Illumination for Two-Dimensional Particle Image Velocimetry, Meas. Sci. Technol., 11 (2000a), 809-814.

Meinhart, C. D., Wereley, S. T. and Santiago, J. G., A PIV Algorithm for Estimating Time-Averaging Velocity Fields, J. Fluids Engineering, 122 (2000b), 285-289.

Nakano, A., Minamiyama, M., Sugii, Y. and Nishio, S., Measurement of Red Cell Velocity Profile in Microvessels Using Particle Image Velocimetory Combined With High-Speed Digital Video Microcirculation Annual, Japanese Society for Microcirculation, 17 (2001), 159-160.

Okamoto, K., Nishio, S., Saga, T. and Kobayashi, T., Standard Images for Particle Imaging Velocimetry, Meas. Sci. Technol. 11 (2000) 685-691.

Olsen, M. G. and Adrian, R. J., Out-Of-Focus Effects on Particle Image Visibility and Correlation in Microscopic Particle Image Velocimetry, Exp. Fluids, Suppl. (2000), S166-S174

Pit, R., Hervert, H. and Leger, L., Direct Experimental Evidence of Slip in Hexadecane: Solid Interface, Physical Review Letters, 85-5 (2000), 980-983.

Raffel, M., Willert, C. E. and Kompenhans, J., Particle Image Velocimetry, Springer. (1998).

Santiago, J. G., Wereley, S. T., Meinhart, C. D., Beebe, D. J. and Adrian, R. J., A Particle Image Velocimetry System for Microfluidics, Exp. Fluids, 25 (1998), 316-319

Seki, J., Sasaki, Y., Oyama, T. and Yamamoto, J., Fiber-Optic Laser-Doppler Anemometer Microscope Applied to the Cerebral Microcirculation in Rats, Biorheology, 33 (1996), 463-470.

Sugii, Y., Nishio, S., Okuno, T. and Okamoto, K., A Highly Accurate Iterative PIV Technique Using Gradient Method, Meas. Sci. Technol., 11 (2000), 1666-1673.

Sugii, Y., Nakano, A., Nishio, S. and Minamiyama, M., Blood Flow Velocity Measurement in Microcirculation Field by Means of Highly Accurate Iterative PIV, Trans. Japan Society of Mechanical Engineers, 67-662 (2001), 2431-2436 (in Japanese).

Sugii, Y., Nishio, S. and Okamoto, K., In Vivo PIV Measurement of Red Blood Cell Velocity Field in Microvessels Considering Mesentery Motion, Physiol. Meas., 23 (2002), 403-416.

Tangelder, G. J., Slaaf, D. W., Muijtjens, A. M. M., Arts, T., oude Egbrink, M. G. A. and Reneman, R. S., Velocity Profiles of Blood Platelets and Red Blood Cells Flowing in Arterioles of the Rabbit Mesentery, Circ. Res., 59 (1986), 505-514.

Tsukada, K., Minamitani, H., Sekizuka, E. and Oshio, C., Image Correlation Method for Measuring Blood Flow Velocity in Microcirculation: Correlation 'Window' Simulation and in Vivo Image Analysis, Physiol. Meas., 21 (2000), 459-471.

Yamaguchi, S., Yamakawa, T. and Niimi, H., Red Cell Velocity and Microvessel Diameter Measurement by a Two Fluorescent Tracer Method Under Epifluorescence Microscopy: Application to Cerebral Microvessels of Cats, Int. J. Microcirc., 11 (1992), 403-416.

Watanabe, K. and Yanur, Mizunuma, H., Slip of Newtonian Fluids at Slid Boundary, JSME Int. J. Series B, 41-3 (1998), 525-529.

Wayland, H. and Johnson, P. C., Erythrocyte Velocity Measurement in Microvessels by Two-Slit Photometric Method, J. Appl. Physiol., 22 (1967), 333-337.

Author Profile

Yasuhiko Sugii: He received his Ph. D degree from Osaka Prefecture University in 2000. He worked in Kao corporation from 1992 to 1995, and he was a post-doctoral fellow in Nuclear Engineering Research Laboratory, University of Tokyo from 2000 to 2002. He works as a research associate in Nuclear Engineering Research Laboratory, University of Tokyo since 2002. His research interests are in the image measurement of flow field, bio-fluid mechanics in blood flow and micro flow dynamics in MEMS and Micro TAS.

Koji Okamoto: He received his MSc(Eng) in Nuclear Engineering in 1985 from University of Tokyo. He also received his Ph.D in Nuclear Engineering in 1992 from University of Tokyo. He worked in Department of Nuclear Engineering, Texas A & M University as a visiting associate professor in 1994. He works in Nuclear Engineering Research Laboratory, University of Tokyo as an associate professor since 1993. His research interests are Quantitative Visualization, PIV, Holographic PIV Flow Induced Vibration and Thermal-hydraulics in Nuclear Power Plant.